



# Third Trimester Fetal Cardiac Blood Flow and Cardiac Outcomes in School-Age Children Assessed By Magnetic Resonance Imaging

Liza Toemen, MD, MSc;\* Gavro Jelic, MD, MSc;\* Marjolein N. Kooijman, MSc; Romy Gaillard, MD, PhD; Willem A. Helbing, MD, PhD; Aad van der Lugt, MD, PhD; Arno A. W. Roest, MD, PhD; Irwin K. M. Reiss, MD, PhD; Eric A. P. Steegers, MD, PhD; Vincent W. V. Jaddoe, MD, PhD

**Background**—An adverse fetal environment leads to fetal hemodynamic adaptations with cardiac flow alterations that may subsequently affect cardiac development. We examined the associations of third trimester placental and fetal cardiac hemodynamics with cardiac outcomes in school-age children.

**Methods and Results**—We performed a population-based prospective cohort study among 547 mothers and their children. At a gestational age of 30.4 (95% range 28.4–32.7) weeks, we measured umbilical and cerebral artery resistance, cardiac output, and tricuspid and mitral E/A waves with Doppler. At the median age of 10.0 years (95% range 9.4–11.7) we measured cardiac outcomes with cardiac magnetic resonance imaging. Cardiac outcomes included right ventricular end-diastolic volume and right ventricular ejection fraction, left ventricular end diastolic volume and left ventricular ejection fraction, left ventricular mass, and left ventricular mass-to-volume ratio as left ventricular mass/left ventricular end diastolic volume. Higher third-trimester umbilical artery resistance was associated with higher childhood right ventricular ejection fraction ( $P$  value  $<0.05$ ), but not with other cardiac outcomes. The third-trimester umbilical artery-cerebral artery pulsatility index ratio was not associated with childhood cardiac outcomes. Higher third-trimester fetal left cardiac output was associated with lower childhood left ventricular ejection fraction and higher left ventricular mass-to-volume ratio ( $P$  value  $<0.05$ ). Third-trimester fetal right cardiac output was not associated with childhood cardiac outcomes. A higher third-trimester fetal tricuspid valve E/A ratio was associated with higher childhood right ventricular ejection fraction ( $P$  value  $<0.05$ ).

**Conclusions**—Our findings suggest that fetal cardiac fetal blood flow redistribution may have long-term effects on cardiac structure and function. These results should be considered as hypothesis generating and need further replication. (*J Am Heart Assoc.* 2019;8:e012821. DOI: 10.1161/JAHA.119.012821.)

**Key Words:** cardiac development • cardiac magnetic resonance imaging • childhood • fetal programming • placental hemodynamics

Cardiovascular disease is at least partially established in the earliest phase of life.<sup>1</sup> Changes in fetal hemodynamics may be a mechanism linking an adverse fetal environment with cardiovascular adaptations and subsequent risk of cardiovascular disease in later life.<sup>2</sup> An adverse fetal environment leads to fetal blood flow redistribution in favor of the upper parts of the body at expense of the trunk, a

phenomenon known as “brain sparing”.<sup>3</sup> This fetal blood flow redistribution also leads to intra-cardiac flow changes with cardiac output switched in favor of the left ventricle, which provides blood for the brain circulation.<sup>4</sup> A rise in the placental vascular resistance and peripheral arterial vasoconstriction in the trunk causes increased right ventricular afterload, and a drop in right cardiac output.<sup>5</sup> The rise in

From the Generation R Study Group (L.T., G.J., M.N.K., R.G., V.W.V.J.), Department of Pediatrics (L.T., G.J., M.N.K., R.G., W.A.H., I.K.M.R., V.W.V.J.), Department of Epidemiology (L.T., G.J., M.N.K., R.G., V.W.V.J.), Department of Radiology (A.v.d.L.), and Department of Obstetrics & Gynecology (E.A.P.S.), Erasmus University Medical Center, Rotterdam, the Netherlands; Department of Pediatrics, Leiden University Medical Center, Leiden, the Netherlands (A.A.W.R.).

Accompanying Data S1, Tables S1 through S3 and Figures S1, S2 are available at <https://www.ahajournals.org/doi/suppl/10.1161/JAHA.119.012821>

\*Dr Toemen and Dr Jelic are co-first authors.

**Correspondence to:** Vincent W. V. Jaddoe, MD, PhD, Generation R Study Group (Na 29-15), Erasmus University Medical Center, Rotterdam, Rotterdam, The Netherlands. E-mail: [v.jaddoe@erasmusmc.nl](mailto:v.jaddoe@erasmusmc.nl)

Received April 5, 2019; accepted July 1, 2019.

© 2019 The Authors. Published on behalf of the American Heart Association, Inc., by Wiley. This is an open access article under the terms of the Creative Commons Attribution-NonCommercial-NoDerivs License, which permits use and distribution in any medium, provided the original work is properly cited, the use is non-commercial and no modifications or adaptations are made.

## Clinical Perspective

### What Is New?

- In a large prospective population-based cohort study involving 547 children, we showed the associations of placenta and fetal cardiac blood flow patterns with childhood right and left cardiac structure and function assessed by magnetic resonance imaging.
- Higher umbilical artery resistance in fetal life was associated with higher childhood right ventricular function.
- Higher fetal left cardiac output was associated with lower childhood left ventricular function and altered cardiac structure.

### What Are the Clinical Implications?

- Cardiac fetal blood flow redistribution may have long-term effects on cardiac structure and function.
- Additional research is necessary to replicate our results and examine the associations of fetal hemodynamics with later cardiac structure and function and with cardiovascular disease risk in adulthood.

ventricular afterload leads to reduced peak systolic velocities in the aorta and pulmonary artery.<sup>6</sup> These changes in intra-cardiac blood flow patterns may affect right and left ventricular structure and function in later life through alterations in shear stress and wall tension, and through the effects on cardiomyocyte maturation and apoptosis.<sup>6</sup> Previously, we reported that lower third-trimester fetal growth was associated with specific fetal hemodynamic changes, such as reduction of cardiac output, stroke volume, and pulmonary artery and cardiac compliance.<sup>7</sup> The long-term consequences of these fetal flow adaptations are not known. A previous study among 200 children reported that fetal growth restriction is associated with cardiac shape and stroke volume alterations in children aged 5 years.<sup>2</sup> In line with these findings, we previously observed that fetal cardiac hemodynamics, mainly uterine artery resistance (UA PI) and left cardiac output in the third trimester, were associated with cardiac dimensions in the first 6 years.<sup>8,9</sup>

Therefore, we examined in a population-based prospective cohort study among 547 children the associations of placenta and fetal cardiac blood flow patterns with childhood right and left cardiac outcomes, assessed by cardiac magnetic resonance imaging (MRI).

## Methods

Data, analytical methods, and study materials will not be made available to other researchers for purposes of reproducing the results or replicating the procedure.

## Study Design

This study was embedded in the Generation R Study, a population-based prospective cohort study from fetal life onwards in Rotterdam, The Netherlands.<sup>10</sup> Details of this study have been described previously.<sup>10</sup> Detailed assessments of fetal growth and blood flow patterns were conducted in a subgroup of 1216 Dutch mothers and their children.<sup>10</sup> Third-trimester fetal hemodynamics were available in 1179 singleton live-born children, of whom 547 visited the Generation R MRI research center at the age of 10 years and did not have cardiac abnormalities (Figure S1). Written consent was received from parents. The study has been approved by the local Medical Ethics Committee.

## Third Trimester Fetal Growth and Hemodynamics Characteristics

In the third trimester, we measured head circumference, abdominal circumference, and femur length and estimated fetal weight using the formula by Hadlock et al.<sup>11</sup> Fetal hemodynamics were assessed by pulsed-wave Doppler at a median gestational age of 30.2 weeks (95% range 28.8–32.3 weeks), as described previously.<sup>7,9</sup> For each measurement, 3 consecutive uniform waveforms were recorded and the mean was used for analyses. Feto-placental vascular resistance was evaluated with recorded flow-velocity waveforms from the umbilical artery. An increase in umbilical artery pulsatility index (UA PI) indicates increased umbilical artery resistance.<sup>7</sup> UA PI was determined in a free-floating loop of the umbilical cord. Color Doppler visualization was used to obtain flow-velocity waveforms of the proximal part of the cerebral arteries. An increased ratio between the UA PI and the middle cerebral artery (MCA) PI is an indicator of brain sparing. This umbilical artery-cerebral artery ratio (U/C ratio) is calculated as UA PI/ MCA PI.<sup>6,9</sup>

Cardiac flow-velocity waveforms at the level of the mitral and tricuspid valves were recorded from the apical 4-chamber view of the fetal heart. Peak velocities of the E wave and the A wave were recorded. The E/A ratio is an index for ventricular diastolic function and expresses both cardiac compliance and preload conditions.<sup>7</sup> A higher E/A ratio reflects less stiff and more compliant ventricles. Cardiac outflow flow-velocity waveforms from the aorta and pulmonary artery were recorded from the 5-chamber view and the short-axis view of the fetal heart just above the semi-lunar valves. Peak systolic velocities in the aorta and pulmonary artery, time-velocity integral, fetal heart rate, and the inner diameters during systole were recorded. Left and right cardiac output were calculated in milliliters per minute by multiplying the vessel area of the aorta or pulmonary artery by the time-velocity integral by fetal heart rate.

## Cardiac Magnetic Resonance Imaging

MRI scanning was performed on a wide-bore GE Discovery MR 750 3T scanner (General Electric, Milwaukee, WI). The scanning environment was introduced to the children in a 30-minute simulated scanning session. Total brain and body scanning session lasted  $\approx 1$  hour, of which 12 minutes was reserved for the cardiac imaging. Briefly, we acquired localizer images, followed by ECG gated breath-held scans lasting  $<10$  seconds per breath-hold (Data S1). A short-axis SSFP cine stack was then obtained with basal slice alignment and covering the ventricles and part of the atria with contiguous 8-mm thick slices over several end expiration breath-holds. The scans were stored on a digital archive for post-processing. Off-line image analyses for right and left ventricular measures on the short-axis cine stack was performed by Precision Image Analysis (Kirkland, WA) under supervision of an experienced radiologist, using Medis QMASS software (Medis, Leiden, The Netherlands). The guidelines of the Society for Cardiovascular Magnetic Resonance (SCMR) were followed to semi-automatically contour right and left ventricular short-axis endocardial and left ventricular epicardial borders.<sup>12</sup> Papillary muscle was included in the ventricular cavity. Cardiac measurements included right ventricular end-diastolic volume (RVEDV), right ventricular ejection fraction (RVEF), left ventricular end diastolic volume (LVEDV), left ventricular ejection fraction (LVEF), and left ventricular mass (LVM). We calculated left ventricular mass-to-volume ratio (LMVR) as  $LVM/LVEDV$ .

## Covariates

We obtained information about gestational age at birth, birth weight, and sex from midwife and hospital records. Information about maternal age, pre-pregnancy body mass index, folic acid use, and smoking during pregnancy, maternal education, and infant breastfeeding was collected by questionnaires and medical charts. At the age of 10 years, child height and weight were measured without shoes and heavy clothing, and body mass index (BMI) and body surface area (BSA) were calculated. BSA was computed using the Haycock formula ( $BSA (m^2) = 0.024265 \times \text{weight (kg)}^{0.5378} \times \text{height (cm)}^{0.3964}$ ).<sup>13</sup> Systolic and diastolic blood pressures were measured on the right brachial artery, using the validated automatic sphygmomanometer Accutorr Plus (Datascop Corporation, Fairfield, New Jersey). These measurements preceded the cardiac MRI by a median of 1.1 months (95% range 0–24.8 months).

## Statistical Analyses

First, we assessed the differences in subject characteristics between boys and girls using ANOVA for continuous variables, Kruskal–Wallis tests for non-parametric variables, and chi-

square tests for categorical variables. Similarly, we compared subject characteristics for children with and without successful cardiac MRI in a non-response analysis. Second, we explored the Pearson correlation coefficients between fetal hemodynamics in third trimester and all childhood cardiac outcomes. Main hemodynamic exposure measures included fetal blood flow redistribution measures (UA PI, U/C ratio), right cardiac measures (right cardiac output, pulmonary artery peak systolic velocity (PSV), tricuspid valve E/A ratio) and left cardiac measures (left cardiac output, aorta ascendens PSV and mitral valve E/A ratio). Childhood cardiac outcomes include RVEDV, RVEF, LVEDV, LVEF, LVM, and LMVR. Third, we used linear regression models to analyze the associations of third trimester fetal hemodynamics and cardiac outcomes at the age of 10 years. Models were adjusted for child sex, gestational age at third trimester measurement, current age and time difference between measurement of BSA and cardiac MRI. Covariates (estimated third trimester fetal weight, maternal age, folic acid intake and smoking status during pregnancy, maternal education level, breast feeding, and childhood blood pressure) were selected on the basis of their associations with the outcomes of interest based on previous study results, but they were not included in the models, because they did not cause a change in effect estimate  $>10\%$ . We did not observe sex-specific interaction with fetal hemodynamics in relationship to the cardiac outcomes of interest. Therefore, we did not stratify our analysis on sex. We constructed BSA-adjusted standard deviation scores (SDS) for the cardiac outcomes using Generalized Additive Models for Location, Size and Shape using R, version 3.2.0 (R Core Team, Vienna, Austria).<sup>14–16</sup> These models enable flexible modeling, taking into account the distribution of the response variable.<sup>17</sup> The SDS of the cardiac outcomes are based on the full cohort of all children who had successful cardiac MRI ( $N=3018$ ), not only on the sub-selection in the current study. Since LMVR is not usually standardized on BSA, we created standard deviation scores as (observed value-mean)/SD. We also created these SDS for all determinants, to enable comparison of effect estimates. To reduce potential bias attributable to missing data, we performed multiple imputations ( $n=5$ ) of missing covariates. We did not adjust for multiple testing, since the different determinants or outcomes are strongly correlated and adjusting for multiple testing might be too strict. For our analyses we used the Statistical Package of Social Sciences version 21.0 (SPSS Inc, Chicago, IL).

## Results

### Subject Characteristics

Subject characteristics are presented in Table 1. At the age of 10 years RVEDV, LVEDV, and LVM were higher in boys than in girls, whereas RVEF and LVEF were slightly higher in girls

**Table 1.** Subject Characteristics (n=547)

	Boys (n=266)	Girls (n=281)	P Value
<b>Maternal characteristics</b>			
Age, y	31.8 (3.8)	32.3 (3.8)	0.18
Prepregnancy BMI, kg/m <sup>2</sup>	22.6 (18.3–32.9)	23.0 (18.8–34.3)	0.18
Folic acid intake during pregnancy, start periconceptional, n (%)	180 (67.7)	189 (67.2)	0.87
Never smoked during pregnancy, n (%)	222 (80.7)	227 (78.5)	0.20
High education level, n (%)	214 (77.8)	213 (73.7)	0.27
<b>Third trimester fetal measurements</b>			
Gestational age at measurement, wk	30.5 (28.6–32.8)	30.4 (28.3–32.7)	0.22
Estimated fetal weight, g	1636 (1194–2236)	1601 (1172–2232)	0.49
<b>Vascular resistance parameters</b>			
Umbilical artery PI	0.95 (0.15)	0.98 (0.17)	0.05
Umbilical/middle cerebral artery ratio	0.50 (0.11)	0.50 (0.11)	0.51
<b>Fetal cardiac hemodynamics</b>			
Right cardiac output, mL/min	822 (244)	833 (226)	0.62
Pulmonary artery PSV, cm/s	72.5 (9.4)	74.1 (9.5)	0.05
Tricuspid valve E/A ratio	0.77 (0.08)	0.78 (0.09)	0.08
Left cardiac output, mL/min	614 (179)	598 (162)	0.28
Aorta ascendens PSV, cm/s	91.0 (12.3)	91.3 (12.3)	0.74
Mitral valve E/A ratio	0.78 (0.1)	0.79 (0.1)	0.16
<b>Birth characteristics</b>			
Gestational age at birth, wk	40.4 (37.0–42.6)	40.1 (37.0–42.1)	<0.01
Birth weight, g	3620 (450)	3469 (512)	<0.01
Breastfeeding, never, n (%)	24 (9.0)	26 (9.2)	0.88
<b>Childhood characteristics</b>			
Age at follow-up, y	10.0 (9.4–11.8)	10.0 (9.4–11.7)	0.41
Height, cm	142.4 (6.4)	142.0 (6.2)	0.53
Weight, kg	33.8 (25.8–50.3)	34.0 (25.1–47.4)	0.34
Body mass index, kg/m <sup>2</sup>	16.6 (13.8–23.0)	17.0 (13.8–22.5)	0.11
Body surface area, m <sup>2</sup>	1.15 (0.96–1.46)	1.16 (0.95–1.42)	0.43
Systolic blood pressure, mm Hg	102 (7)	104 (7.7)	<0.01
Diastolic blood pressure, mm Hg	57 (6)	58 (6)	<0.01

Values represent means (SD), medians (95% range) or numbers of subjects (valid %) and are based on imputed data. Differences in subject characteristics between groups were evaluated using one-way ANOVA tests or Kruskal–Wallis tests for continuous variables and chi-square tests for proportions. BMI indicates body mass index; PI, pulsatility index; PSV, peak systolic velocity.

(Table 2). These measures were also different between boys and girls when standardized on BSA (Table S1). The correlations of placental and fetal cardiac hemodynamics with childhood cardiac outcomes (standardized on BSA) are shown in Table S2. The correlation between UA PI and RVEF is visualized in Figure S2. A non-response analysis is shown in Table S3. Children with successful cardiac MRIs had mothers who were older, had higher intake of periconceptional folic acid, smoked less frequently during pregnancy, and were

more often higher educated. There were no differences in fetal hemodynamics and childhood anthropometric measures between children with and without follow-up studies.

### Fetal Hemodynamics and Left and Right Cardiac Outcomes

Table 3 shows that a 1-SDS increase in third trimester UA PI was associated with higher childhood RVEF (0.11 SDS [95%

**Table 2.** Childhood Cardiac Outcomes (n=547)

	Boys	Girls	P Value
Right cardiac outcomes			
Right ventricular end diastolic volume, mL	105.6 (18.7)	95.8 (17.1)	<0.01
Right ventricular ejection fraction, %	58.0 (4.9)	60.0 (5.0)	<0.01
Left cardiac outcomes			
Left ventricular end diastolic volume, mL	104.8 (16.5)	96.7 (14.9)	<0.01
Left ventricular ejection fraction, %	58.3 (4.6)	59.3 (4.5)	0.01
Left ventricular mass, g	50.6 (9.9)	46.5 (10.0)	<0.01
Left ventricular mass-to-volume ratio, g/mL	0.49 (0.08)	0.48 (0.08)	0.60

Values represent means (SD). Differences in subject characteristics between groups were evaluated using one-way ANOVA tests. Cardiac outcomes standardized on body surface area are shown in Table S1.

CI 0.02–0.20]). UA PI was not associated with any of the other cardiac outcomes. The U/C ratio was not associated with childhood cardiac outcomes.

Table 4 shows that right cardiac output and pulmonary artery PSV were not associated with childhood right ventricular outcomes. However, a 1-SDS higher fetal tricuspid valve E/A ratio, reflecting a less stiff and more compliant ventricle, was associated with higher childhood RVEF (0.09 [95% CI 0.00–0.17]).

Table 5 shows that a higher fetal left cardiac output was associated with lower childhood LVEF (−0.15 [95% CI −0.24–0.05]) and higher LMVR (0.11 [95% CI 0.01–0.20]). Aorta ascendens PSV and mitral valve E/A wave were not associated with childhood left ventricular outcomes.

## Discussion

In this prospective cohort study, we observed that a higher UA PI, reflecting increased arterial resistance, was associated with higher childhood RVEF. A lower fetal tricuspid valve E/A

ratio, indicating a stiffer and less compliant ventricle, was associated with a lower childhood RVEF. Higher fetal left cardiac output was associated with lower childhood LVEF and higher childhood LMVR.

## Interpretation of Main Findings

Changes in fetal hemodynamics in response to an adverse fetal environment may lead to cardiovascular adaptations and subsequent risk of cardiovascular disease in later life.<sup>2</sup> We previously reported that among 1215 fetuses decreased fetal growth was associated with a higher afterload and lower vascular compliance, even before the apparent stage of fetal growth restriction.<sup>7</sup> These adaptations might lead to cardiac changes in structure and function in later life. Also, in the same cohort it was reported that a higher UA PI was associated with lower aortic root diameter at 2 years and with lower LVM at 6 years.<sup>8,9</sup> Increased fetal left cardiac output was associated with larger LVM and atrial diameter at 2 years and with larger aortic root diameter at 6 years.<sup>8,9</sup> Another

**Table 3.** Associations of Fetal Blood Flow Redistribution With Childhood Right and Left Cardiac Outcomes (n=547)

Fetal Blood Flow Redistribution Exposures (SDS)	Childhood Cardiac Outcomes (SDS)					
	Right Ventricular End-Diastolic Volume	Right Ventricular Ejection Fraction	Left Ventricular End-Diastolic Volume	Left Ventricular Ejection Fraction	Left Ventricular Mass	Left Ventricular Mass-To-Volume Ratio
Umbilical artery PI	−0.05 (−0.13 to 0.02)	0.11 (0.02 to 0.20)*	−0.03 (−0.10 to 0.04)	0.06 (−0.03 to 0.15)	−0.04 (−0.12 to 0.04)	−0.01 (−0.09 to 0.08)
Umbilical/cerebral ratio	−0.06 (−0.13 to 0.02)	0.08 (−0.02 to 0.17)	−0.05 (−0.13 to 0.02)	0.09 (−0.00 to 0.18)	−0.01 (−0.09 to 0.07)	0.04 (−0.06 to 0.13)

Values are regression coefficients (95% CI) from linear regression models that reflect differences of childhood right and left ventricular outcomes in SDS per SDS change in fetal blood flow redistribution exposures. Cardiac measures at 10 years are standardized on body surface area (except left ventricular mass-to-volume ratio). Model is adjusted for gestational age at third trimester measurement, child sex, current age, and time difference between measurement of body surface area and magnetic resonance imaging. PI indicates pulsatility index; SDS standard deviation score.

\* $P<0.05$ .



**Table 4.** Associations of Right Sided Fetal Hemodynamics on Childhood Right Ventricular Outcomes (n=547)

Fetal Right Cardiac Blood Flow Exposures (SDS)	Childhood Right Ventricular Outcomes (SDS)	
	Right Ventricular End-Diastolic Volume	Right Ventricular Ejection Fraction
Right cardiac output	−0.03 (−0.11 to 0.06)	0.06 (−0.04 to 0.16)
Pulmonary artery PSV	−0.03 (−0.11 to 0.04)	0.04 (−0.05 to 0.14)
Tricuspid valve E/A wave	−0.02 (−0.09 to 0.06)	0.09 (0.00 to 0.17)*

Values are regression coefficients (95% CI) from linear regression models that reflect differences of childhood right ventricular outcomes in SDS per SDS change in cardiac blood flow exposures. Cardiac measures at 10 years are standardized on body surface area. Model is adjusted for gestational age at third trimester measurement, child sex, current age, and time difference between measurement of body surface area and magnetic resonance imaging. PSV indicates peak systolic velocity; SDS, standard deviation score.

\* $P<0.05$ .

study among 200 children aged 3 to 6 years, observed that small for gestational age children have a more globular heart, impaired relaxation, and increased blood pressure and intima-media thickness.<sup>18</sup> Thus, previous studies suggest that fetal growth is associated with fetal blood flow alterations and that these changes might be associated with left cardiac structural and functional outcomes in childhood. Another study in preterm born young adults showed that changes in right ventricular structure and function were more pronounced in the right ventricle than in the left.<sup>19</sup> Thus far, no studies on the long-term effects of fetal hemodynamics have been performed in children aged >6 years. Also, no information is available on structural developmental adaptations of the right ventricle.

In the current study, we did not find associations of fetal UA PI with LVM at the age of 10 years. Possibly, the previously observed association of UA PI with LVM at 6 years is transient and disappears at older age. In the current study, we did observe an association of UA PI with childhood cardiac function. Previous research in children with fetal growth restriction showed reduced longitudinal motion and impaired relaxation, but no difference in ejection fraction.<sup>20</sup> We observed that a higher UA PI was associated with higher RVEF. These findings may suggest that a higher umbilical artery resistance, reflecting a higher fetal right ventricular afterload, is associated with higher childhood RVEF. A study in

growth restricted fetuses observed an increased venous return in the superior vena cava, as a result of increased cerebral flow in brain sparing.<sup>21</sup> This might also affect right ventricular function. However, we did not observe associations of U/C ratio or right cardiac output with childhood RVEF. Further studies are needed to replicate these findings. We also hypothesized that since a higher U/C ratio, reflecting brain sparing, is associated with lower cardiac output in fetal life, it would also be associated with reduced childhood right and left ejection fraction.<sup>3</sup> However, in the current study we did not observe any associations of U/C ratio with childhood cardiac structure or function, independent of current BSA.

Reduced fetal growth across the full range is associated with lower fetal right and left cardiac output, aorta ascendens and pulmonary artery PSV and possibly with lower E/A ratio's.<sup>3,6,7,22</sup> To the best of our knowledge, there are no other studies on the associations of fetal cardiac output with childhood cardiac outcomes. We observed that higher fetal left cardiac output was associated with lower childhood LVEF and higher LMVR, but not with LVEDV or LVM. We also observed that lower fetal tricuspid valve E/A ratio was associated with lower RVEF. A lower E/A ratio indicates a less compliant ventricle and therefore worse diastolic function. Interestingly, in our study the lower diastolic function in fetal life was associated with lower childhood ejection fraction, an indicator of systolic function. Unfortunately, we did not have

**Table 5.** Associations of Left Sided Fetal Hemodynamics on Childhood Left Ventricular Outcomes (n=547)

Fetal Left Cardiac Blood Flow Exposures (SDS)	Childhood Left Ventricular Outcomes (SDS)			
	Left Ventricular End-Diastolic Volume	Left Ventricular Ejection Fraction	Left Ventricular Mass	Left Ventricular Mass-To-Volume Ratio
Left cardiac output	0.00 (−0.08 to 0.08)	−0.15 (−0.24 to −0.05)*	0.09 (0.00 to 0.17)	0.11 (0.01 to 0.20) <sup>†</sup>
Aorta ascendens PSV	−0.07 (−0.14 to 0.01)	−0.05 (−0.14 to 0.04)	−0.01 (−0.09 to 0.07)	0.04 (−0.05 to 0.13)
Mitral valve E/A wave	−0.01 (−0.07 to 0.06)	0.02 (−0.06 to 0.10)	0.06 (−0.02 to 0.13)	0.06 (−0.03 to 0.14)

Values are regression coefficients (95% CI) from linear regression models that reflect differences of childhood left ventricular outcomes in SDS per SDS change in fetal cardiac blood flow exposures. Cardiac measures at 10 years are standardized on body surface area (except left ventricular mass-to-volume ratio). Model is adjusted for gestational age at third trimester measurement, child sex, current age, and time difference between measurement of body surface area and magnetic resonance imaging. PI indicates pulsatility index; PSV peak systolic velocity; SDS standard deviation score.

\* $P<0.01$ ; <sup>†</sup> $P<0.05$ .

childhood diastolic cardiac filling measures. We did not observe associations of mitral valve E/A ratio with left cardiac structure or function at the age of 10 years.

Most of the associations we observed could fit the hypothesis that changes in fetal hemodynamics could be associated with cardiac structure and function in later life, putting the individual at risk for cardiovascular disease. The observed associations could reflect chance findings. We did not take into account multiple testing because our different exposures and outcomes are strongly correlated, and adjusting for multiple testing might be too strict. Also, we studied women with relatively healthy pregnancies. It might be possible that in more compromised pregnancies fetal hemodynamic adaptations influence later cardiac structure and function more strongly.

## Methodological Considerations

The main strength of this study is the prospective design from early fetal life onwards, in a large cohort of children. To our knowledge, this is the first study examining the effects of fetal hemodynamics on cardiac outcomes, measured by cardiac MRI in childhood. MRI is a more precise and accurate tool than ultrasound and CT to study cardiac structure.<sup>23,24</sup> For the current subgroup study, follow up was available in 46%. Missing cardiac MRI scans were mostly because of later start of these measurements during the follow up visits, poor quality cardiac MRI scans were often caused by logistical or participant constraints. This loss to follow-up could lead to bias if the associations of fetal hemodynamics with cardiac measures differ between those included and not included in the analyses. However, we deem this unlikely since non-response analysis showed no differences in fetal hemodynamics or childhood anthropometrics (Table S3). We have standardized our outcomes on BSA, to take into account current body size. The majority of the children visited the MRI within 2 months after anthropometrics were taken. A small proportion of children was invited to the MRI at a later age. For these children, the BSA we calculated might underestimate current body size, leading to increased z-scores for the cardiac outcomes. We adjusted all our analyses for the time difference between the BSA measurement and the MRI visit, but this measurement error could still lead to an attenuation of the effect estimates we observed. Despite the fact that we tested and adjusted for confounders, residual confounding might be of concern, as in any other observational study.

## Conclusions

We observed associations of increased placental resistance and fetal hemodynamics with childhood cardiac

structure and function. Our findings suggest that cardiac fetal blood flow redistribution may have long term effects on cardiac structure and function. These results should be considered as hypothesis generating and need further replication.

## Acknowledgments

We gratefully acknowledge the contribution of children and parents, general practitioners, hospitals, midwives, and pharmacies in Rotterdam.

## Sources of Funding

The Generation R Study is made possible by financial support from the Erasmus Medical Centre, Rotterdam, the Erasmus University Rotterdam and the Netherlands Organization for Health Research and Development. Research that has led to these findings received support by a Netherlands Organization for Health Research and Development grant (VIDI 016.136.361), a European Research Council Consolidator Grant (ERC-2014-CoG-648916). Dr Gaillard received funding from the Dutch Heart Foundation (grant number 2017T013), the Dutch Diabetes Foundation (grant number 2017.81.002) and the Netherlands Organization for Health Research and Development (NWO, ZonMW, grant number 543003109).

## Disclosures

None.

## References

1. Hanson MA, Gluckman PD. Early developmental conditioning of later health and disease: Physiology or pathophysiology? *Physiol Rev*. 2014;94:1027–1076.
2. Crispi F, Bijlens B, Figueras F, Bartrons J, Eixarch E, Le Noble F, Ahmed A, Gratacos E. Fetal growth restriction results in remodeled and less efficient hearts in children. *Circulation*. 2010;121:2427–2436.
3. Rizzo G, Arduini D. Fetal cardiac function in intrauterine growth retardation. *Am J Obstet Gynecol*. 1991;165:876–882.
4. Figueras F, Puerto B, Martinez JM, Cararach V, Vanrell JA. Cardiac function monitoring of fetuses with growth restriction. *Eur J Obstet Gynecol Reprod Biol*. 2003;110:159–163.
5. Severi FM, Rizzo G, Bocchi C, D'Antona D, Verzuri MS, Arduini D. Intrauterine growth retardation and fetal cardiac function. *Fetal Diagn Ther*. 2000;15:8–19.
6. Cohen E, Wong FY, Horne RS, Yiallourou SR. Intrauterine growth restriction: Impact on cardiovascular development and function throughout infancy. *Pediatr Res*. 2016;79:821–830.
7. Verburg BO, Jaddoe VW, Wladimiroff JW, Hofman A, Witteman JC, Steegers EA. Fetal hemodynamic adaptive changes related to intrauterine growth: The generation r study. *Circulation*. 2008;117:649–659.
8. Geelhoed JJ, Steegers EA, van Osch-Gevers L, Verburg BO, Hofman A, Witteman JC, van der Heijden AJ, Helbing WA, Jaddoe VW. Cardiac structures track during the first 2 years of life and are associated with fetal growth and hemodynamics: The generation r study. *Am Heart J*. 2009;158:71–77.
9. Kooijman MN, de Jonge LL, Steegers EA, van Osch-Gevers L, Verburg BO, Hofman A, Helbing WA, Jaddoe VW. Third trimester fetal hemodynamics and cardiovascular outcomes in childhood: The generation r study. *J Hypertens*. 2014;32:1275–1282.

10. Jaddoe VW, Mackenbach JP, Moll HA, Steegers EA, Tiemeier H, Verhulst FC, Witteman JC, Hofman A. The generation r study: Design and cohort profile. *Eur J Epidemiol*. 2006;21:475–484.
11. Hadlock FP, Harrist RB, Carpenter RJ, Deter RL, Park SK. Sonographic estimation of fetal weight. The value of femur length in addition to head and abdomen measurements. *Radiology*. 1984;150:535–540.
12. Schulz-Menger J, Bluemke DA, Bremerich J, Flamm SD, Fogel MA, Friedrich MG, Kim RJ, von Knobelsdorff-Brenkenhoff F, Kramer CM, Pennell DJ, Plein S, Nagel E. Standardized image interpretation and post processing in cardiovascular magnetic resonance: Society for cardiovascular magnetic resonance (scmr) board of trustees task force on standardized post processing. *J Cardiovasc Magn Reson*. 2013;15:35.
13. Lopez L, Colan SD, Frommelt PC, Ensing GJ, Kendall K, Younoszai AK, Lai WW, Geva T. Recommendations for quantification methods during the performance of a pediatric echocardiogram: A report from the pediatric measurements writing group of the american society of echocardiography pediatric and congenital heart disease council. *J Am Soc Echocardiogr*. 2010;23:465–495; quiz 576–467.
14. National High Blood Pressure Education Program Working Group on High Blood Pressure in C, Adolescents. The fourth report on the diagnosis, evaluation, and treatment of high blood pressure in children and adolescents. *Pediatrics*. 2004;114:555–576.
15. Pettersen MD, Du W, Skeens ME, Humes RA. Regression equations for calculation of z scores of cardiac structures in a large cohort of healthy infants, children, and adolescents: An echocardiographic study. *J Am Soc Echocardiogr*. 2008;21:922–934.
16. Cantinotti M, Scalese M, Murzi B, Assanta N, Spadoni I, De Lucia V, Crocetti M, Cresti A, Gallotta M, Marotta M, Tyack K, Molinaro S, Iervasi G. Echocardiographic nomograms for chamber diameters and areas in caucasian children. *J Am Soc Echocardiogr*. 2014;27:1279–1292.e2.
17. Rigby RA, Stasinopoulos DM. Generalized additive models for location, scale and shape. *J Roy Stat Soc: Ser C (Appl Stat)*. 2005;54:507–554.
18. Crispi F, Figueras F, Cruz-Lemini M, Bartrons J, Bijnens B, Gratacos E. Cardiovascular programming in children born small for gestational age and relationship with prenatal signs of severity. *Am J Obstet Gynecol*. 2012;207:121.e1–121.e9.
19. Lewandowski AJ, Bradlow WM, Augustine D, Davis EF, Francis J, Singhal A, Lucas A, Neubauer S, McCormick K, Leeson P. Right ventricular systolic dysfunction in young adults born preterm. *Circulation*. 2013;128:713–720.
20. Sarvari SI, Rodriguez-Lopez M, Nunez-Garcia M, Sitges M, Sepulveda-Martinez A, Camara O, Butakoff C, Gratacos E, Bijnens B, Crispi F. Persistence of cardiac remodeling in preadolescents with fetal growth restriction. *Circ Cardiovasc Imaging*. 2017;10:e005270.
21. Zhu MY, Milligan N, Keating S, Windrim R, Keunen J, Thakur V, Ohman A, Portnoy S, Sled JG, Kelly E, Yoo SJ, Gross-Wortmann L, Jaeggi E, Macgowan CK, Kingdom JC, Seed M. The hemodynamics of late-onset intrauterine growth restriction by mri. *Am J Obstet Gynecol*. 2016;214:367.e1–367.e17.
22. Crispi F, Hernandez-Andrade E, Pelsers MM, Plasencia W, Benavides-Serralde JA, Eixarch E, Le Noble F, Ahmed A, Glatz JF, Nicolaides KH, Gratacos E. Cardiac dysfunction and cell damage across clinical stages of severity in growth-restricted fetuses. *Am J Obstet Gynecol*. 2008;199:254.e1–254.e8.
23. Vogel M, Gutberlet M, Dittrich S, Hosten N, Lange PE. Comparison of transthoracic three dimensional echocardiography with magnetic resonance imaging in the assessment of right ventricular volume and mass. *Heart*. 1997;78:127–130.
24. Helbing WA, Bosch HG, Maliapaard C, Rebergen SA, van der Geest RJ, Hansen B, Ottenkamp J, Reiber JH, de Roos A. Comparison of echocardiographic methods with magnetic resonance imaging for assessment of right ventricular function in children. *Am J Cardiol*. 1995;76:589–594.



# **Supplemental Material**

## **Data S1.**

### **Supplemental Methods**

#### **Cardiac Magnetic Resonance Imaging**

We performed cardiac magnetic resonance imaging (cMRI) using a wide-bore GE Discovery MR 750 3T scanner (General Electric, Milwaukee, MI, USA). Children were first introduced with the scanning environment through the use of a simulated scanning session. Approximately 60 minutes were reserved for scanning of the brain, lungs, heart, abdomen and hips. Scanning time allocated to the cardiac imaging was 12 minutes. We used multi-phase ungated free-breathing steady-state-free-precession (SSFP) real-time scans to acquire localizer images in all necessary orientations. From these, 2-chamber and 4-chamber views were acquired with ECG gated breath-held scans lasting less than 10 seconds per breath-hold. A short-axis SSFP cine stack was then obtained with basal slice alignment and covering the ventricles and part of the atria with contiguous 8-mm thick slices over several breath-holds. All breath-held cMRI sequences were retrospectively ECG gated with the help of a precordial 4-lead ECG using the vectocardiogram gating option of the patient monitoring unit and acquired at end-expiration. The imaging parameters for the short axis acquisitions were as follow: field of view of 280 x 280 mm<sup>2</sup>, scan matrix of 128 x 128; 16 views per segment, repetition time 3.7 ms, echo time 1.7 ms, flip angle 45°. The 2-chamber, 4-chamber and the short axis SSFP scans were stored on a digital archive for post-processing.

Off-line image analyses for right and left ventricular measures on the short-axis cine stack was performed by Precision Image Analysis (Kirkland, WA, USA) under supervision of an experienced radiologist, using Medis QMASS software (Medis, Leiden, the Netherlands). Right and left ventricular short-axis endocardial and left ventricular epicardial borders were semi-automatically contoured at end-diastole and end-systole to allow automated calculation of right and left ventricular volume and left ventricular mass (LVM), following the guidelines of the Society for Cardiovascular Magnetic Resonance (SCMR).(1) Papillary muscle was included in the ventricular cavity. LVM was calculated as (diastolic epicardial volume-diastolic endocardial volume)×1.05. Since the scan spatial resolution was not adequate

to contour right ventricular epicardial borders, no right ventricular mass could be calculated. Cardiac measurements included right ventricular end-diastolic volume (RVEDV), right ventricular ejection fraction (RVEF), left ventricular end-diastolic volume (LVEDV), left ventricular ejection fraction (LVEF), and LVM. Coefficients of variation were calculated in a random subset of 25 scans. Intra-observer variability was between 2.5% and 7.2%, while interobserver was between 3.5% and 8.7%. Intra-observer variability for each measurement were as follows: RVEDV 3.9%; RVEF 5.1%; LVEDV 2.5%; LVEF 4.3% and LVM 7.2%. Inter-observer variability was: RVEDV 5.0%; RVEF 5.3%; LVEDV 3.5%; LVEF 5.9% and LVM 8.7%.

**Table S1. Childhood cardiac outcomes standardized on body surface area (N=547).**

	Boys	Girls	P-value
<b>Right cardiac outcomes</b>			
Right ventricular end diastolic volume, SDS	0.37 (0.91)	-0.26 (0.89)	<0.01
Right ventricular ejection fraction, SDS	-0.05 (0.99)	0.36 (1.01)	<0.01
<b>Left cardiac outcomes</b>			
Left ventricular end diastolic volume, SDS	0.35 (0.89)	-0.26 (0.86)	<0.01
Left ventricular ejection fraction, SDS	-0.02 (1.01)	0.19 (0.98)	0.14
Left ventricular mass, SDS	0.24 (0.91)	-0.33 (1.04)	<0.01
Left ventricular mass-to-volume ratio, SDS	0.02 (0.96)	-0.02 (1.04)	0.60

SDS Standard Deviation Score; SD standard deviation; Values represent mean SDS (SD). Differences in subject characteristics between groups were evaluated using one-way-ANOVA-tests. Since left ventricular mass-to-volume ratio is not usually standardized on body surface area, we created standard deviation scores as (observed value-mean)/SD.

**Table S2. Correlation coefficients between placental vascular resistance, fetal cardiac hemodynamics and childhood cardiac outcomes.**

	Childhood cardiac outcomes (SDS)					
	RVEDV	RVEF	LVEDV	LVEF	LVM	LMVR
<b>Placental vascular resistance (SDS)</b>						
Umbilical artery PI	-0.10*	0.11*	-0.08	0.06	-0.09*	-0.03
Umbilical/middle cerebral artery ratio	-0.08	0.07	-0.08	0.08	-0.04	0.02
<b>Fetal cardiac hemodynamics (SDS)</b>						
Right cardiac output	0.02	0.07	0.10*	0.00	0.25**	0.20**
Pulmonary artery PSV	-0.02	-0.06	0.02	-0.01	0.09	0.08
Tricuspid valve E/A ratio	-0.02	0.10*	-0.03	0.08	0.03	0.06
Left cardiac output	0.01	0.01	0.09	-0.12**	0.19**	0.14**
Aorta ascendens PSV	-0.07	0.04	0.03	-0.05	0.03	0.04
Mitral valve E/A ratio	-0.04	0.06	-0.02	0.04	0.04	0.05
<b>Childhood cardiac outcomes (SDS)</b>						
RVEDV	1	-0.34**	0.86**	0.04	0.44**	-0.22**
RVEF		1	-0.15**	0.62**	-0.07	0.05
LVEDV			1	-0.13**	0.50**	-0.28**
LVEF				1	-0.01	0.09**
LVM					1	0.68**
LMVR						1

SDS standard deviation scores; PI pulsatility index; PSV peak systolic velocity; RVEDV right ventricular end diastolic volume; RVEF right ventricular ejection fraction; LVEDV left ventricular end diastolic volume; LVEF left ventricular ejection fraction; LVM left ventricular mass; LMVR left ventricular mass-to-volume ratio.

Values represent Pearson correlation coefficients. Cardiac measures at 10 years are standardized on body surface area (except LMVR).

\* P-value<0.05; \*\* P-value<0.01



**Table S3. Non-response analysis (N=1,179).**

	<b>Children without cardiac MRI (n=632)</b>	<b>Children with cardiac MRI (n=547)</b>	<b>P value</b>
<b>Maternal characteristics</b>			
Age, years	31.1 (4.4)	32.1 (3.7)	<0.01
Prepregnancy BMI, kg/m <sup>2</sup>	22.3 (18.4, 34.4)	22.6 (18.6, 34.6)	0.52
Folic acid intake during pregnancy, start periconceptional, n (%)	298 (57)	300 (67)	<0.01
Never smoked during pregnancy, n (%)	417 (72)	392 (79)	0.02
High education level, n (%)	390 (66)	388 (76)	<0.01
<b>Third trimester fetal measurements</b>			
Gestational age at measurement, weeks	30.3 (28.5, 32.6)	30.4 (28.4, 32.7)	0.12
Estimated fetal weight, grams	1601 (1155, 2235)	1618 (1181, 2229)	0.42
<b>Vascular resistance parameters</b>			
Umbilical artery PI	0.98 (0.17)	0.96 (0.16)	0.10
Umbilical/middle cerebral artery ratio	0.51 (0.12)	0.50 (0.11)	0.24
<b>Fetal cardiac hemodynamics</b>			
Right cardiac output, ml/min	850 (259)	825 (234)	0.11
Pulmonary artery PSV, cm/s	73.9 (9.4)	73.4 (9.5)	0.39
Tricuspid valve E/A ratio	0.77 (0.08)	0.78 (0.09)	0.74
Left cardiac output, ml/min	608 (179)	606 (170)	0.84
Aorta ascendens PSV, cm/s	91.4 (12.4)	91.1 (12.3)	0.64
Mitral valve E/A ratio	0.78 (0.10)	0.78 (0.10)	0.46
<b>Birth characteristics</b>			
Gestational age at birth, weeks	40.1 (34.9, 42.4)	40.3 (37.0, 42.4)	0.07
Birth weight, grams	3485 (573)	3544 (491)	0.06
Breastfeeding, never, n (%)	69 (12)	45 (8)	0.04
<b>Childhood characteristics</b>			
Age at follow up, years	10.0 (9.2, 11.7)	10.0 (9.4, 11.7)	0.41
Height, cm	142.7 (6.5)	142.2 (6.3)	0.23
Weight, kg	33.6 (26.2, 50.1)	34.0 (25.3, 48.7)	0.77
Body mass index, kg/m <sup>2</sup>	16.6 (14.0, 22.5)	16.8 (13.8, 22.6)	0.20
Body surface area, m <sup>2</sup>	1.15 (0.98, 1.45)	1.15 (0.96, 1.44)	0.99
Systolic blood pressure, mmHg	103.2 (7.9)	102.9 (7.5)	0.60
Diastolic blood pressure, mmHg	58.3 (6.3)	57.9 (6.3)	0.33

n; number; SD standard deviation; BPM beats per minute; PI pulsatility index; PSV peak systolic velocity. Values represent means (SD), medians (95% range) or numbers of subjects (valid %) and are based on original data. Differences in subject characteristics between groups were evaluated using one-way-ANOVA-tests or Kruskal-Wallis tests for continuous variables and Chi-square tests for proportions.

**Figure S1. Flow chart of the study population.**

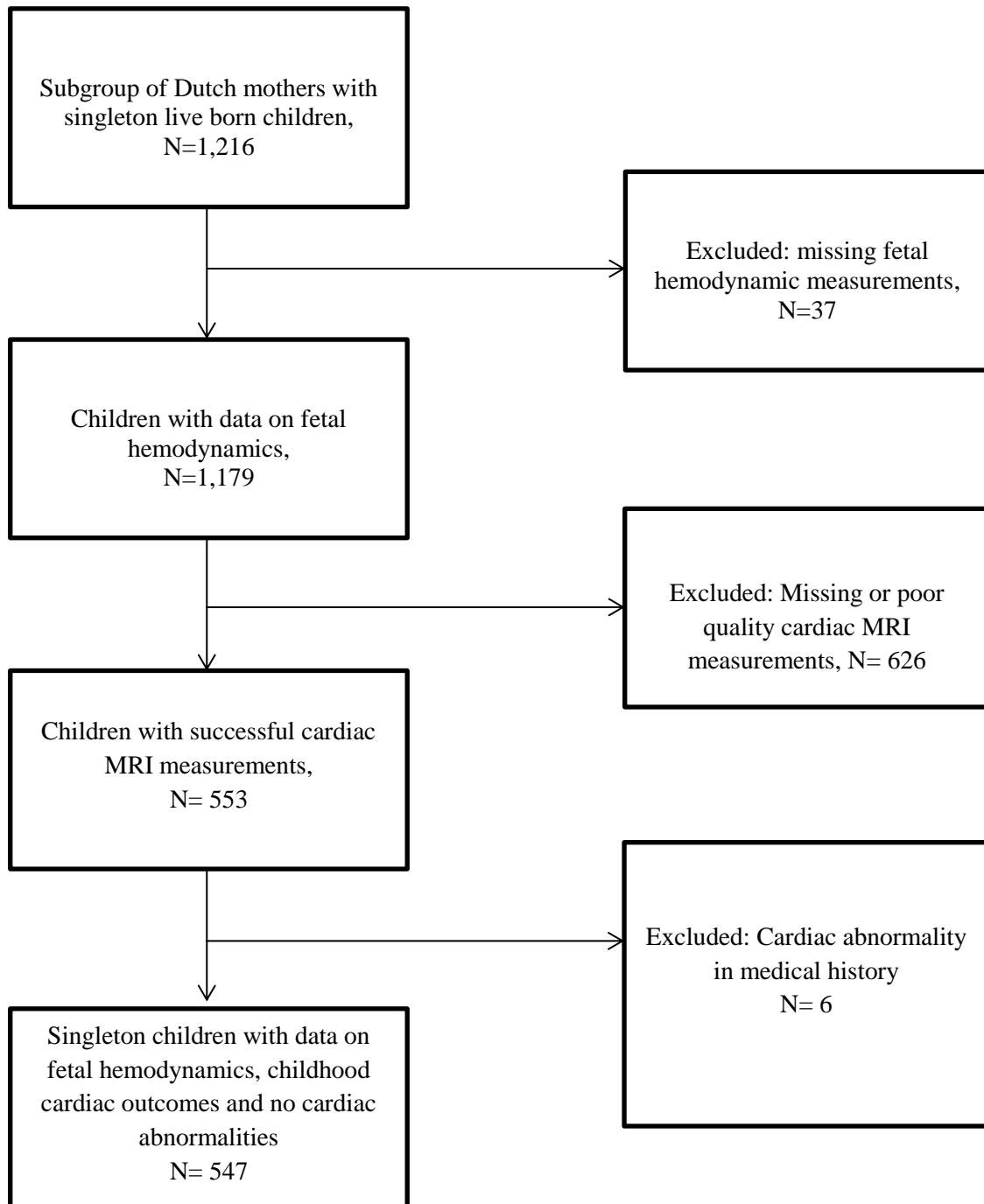
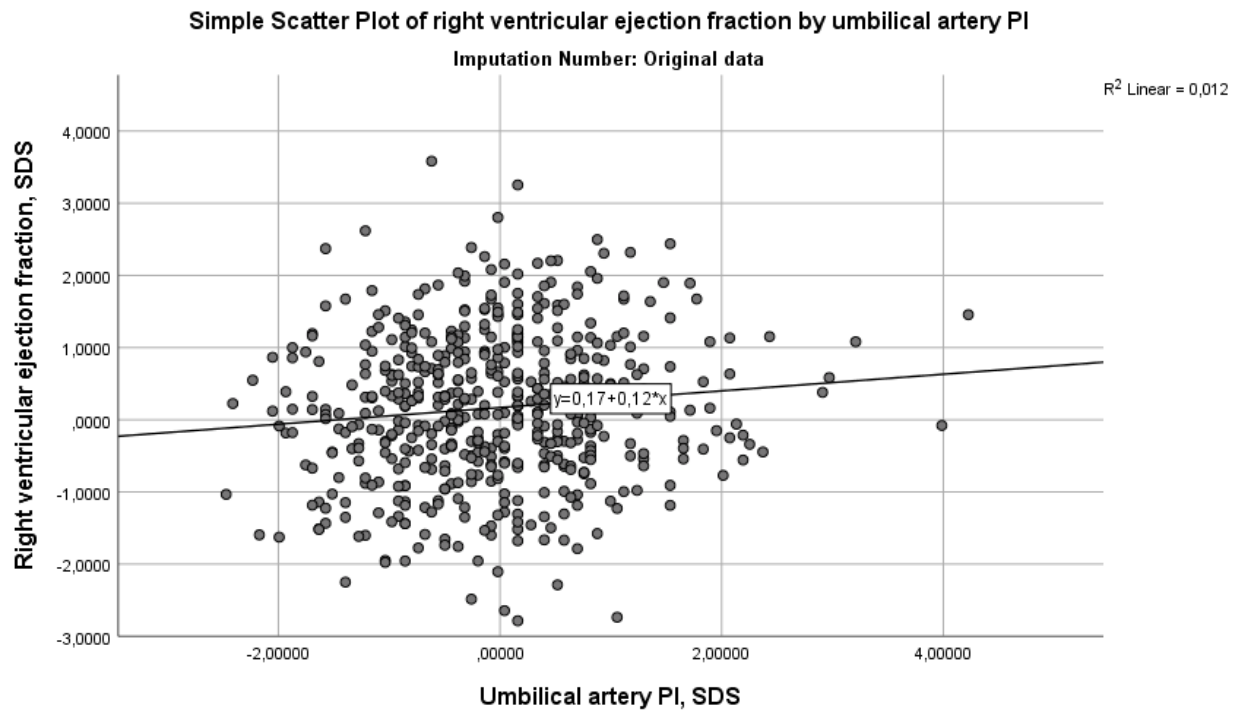


**Figure S2. Correlation scatter plot of right ventricular ejection fraction by umbilical artery PI.**



SDS Standard Deviation Score; PI pulsatility index.

**Supplemental Reference:**

1. Schulz-Menger J, Bluemke DA, Bremerich J, Flamm SD, Fogel MA, Friedrich MG, Kim RJ, von Knobelsdorff-Brenkenhoff F, Kramer CM, Pennell DJ, Plein S, Nagel E. Standardized image interpretation and post processing in cardiovascular magnetic resonance: Society for Cardiovascular Magnetic Resonance (SCMR) board of trustees task force on standardized post processing. *J Cardiovasc Magn Reson*. 2013;15:35.